Structural and Functional Significance of Inhomogeneous Line Broadening of Band III in Hemoglobin and Fe-Mn Hybrid Hemoglobins†

M. D. Chavez,‡ S. H. Courtney,§ M. R. Chance,§,⊥ D. Kiula,∥ J. Nocek,∥ B. M. Hoffman,∥ J. M. Friedman,*,§ and M. R. Ondrias‡

Department of Chemistry, University of New Mexico, Albuquerque, New Mexico 78131, AT&T Bell Laboratories, Murray Hill, New Jersey 07974, Department of Chemistry, New York University, New York, New York 10003, and Department of Chemistry, Northwestern University, Evanston, Illinois 60021

Received August 29, 1989; Revised Manuscript Received January 2, 1990

ABSTRACT: Near-infrared spectra of hemoglobin and Fe-Mn hybrid hemoglobins have been obtained at cryogenic temperatures. The charge-transfer ($a_{2u}(\pi) \rightarrow d_{zy}$) transition at ~760 nm (band III) has been found to be a conformationally sensitive indicator of the heme-pocket geometry in these species. Temperature, protein tertiary and quaternary structure, chain heterogeneity, and ligand rebinding subsequent to CO photolysis all affect the line width and position of this transition. We conclude that the overall line shape of band III is derived from both subunit heterogeneity and conformational disorder within each subunit. A model is suggested that relates the observed pH dependence of the kinetic hole burning due to ligand rebinding to specific structural parameters of the proximal heme pocket that influence both the peak position and the inhomogeneous line shape of band III.

Characterization of the relationship between local protein structures and the functionality of protein active sites continues to pose one of the fundamental challenges in modern biophysics. During the past 2 decades, considerable progress has been made in defining the equilibrium properties of the active sites in heme proteins, particularly hemoglobins and myoglobins. However, the aspects of the active-site structures that determine the functional mechanisms of these systems are only now being defined. It is of particular interest to identify spectroscopic probes of the heme moiety that can be linked to both the local heme-pocket environment and the dynamics of the active site during functional processes. Ideally, such probes should have several characteristics: (1) sensitivity both to local structure at the active site and to states of reactivity, including ligation and oxidation state, (2) responsiveness to overall protein conformational changes that are functionally relevant, and (3) time-dependent behavior reflective of protein dynamics.

Band III in the near-infrared absorption spectra of heme proteins possesses these necessary characteristics and thus offers a versatile probe of the ligand binding sites of heme proteins. This charge-transfer transition at ~760 nm is observed for five-coordinate ferrous hemes but is absent in the spectra of six-coordinate species (Eaton et al., 1981). On the basis of polarized single-crystal absorption, circular dichroism, and magnetic circular dichroism studies, Eaton et al. (1978) assigned the ≈760-nm line of hemoglobin as a z-polarized charge-transfer transition between the porphyrin π system and the iron π system [$a_{2u}(\pi)$-d_{zy}].

The sensitivity of band III to ligation-induced structural changes in cryogenically trapped samples has been demonstrated by several groups (Iizuka et al., 1974; Campbell et al., 1987; Ansari et al., 1985; Fiamingo et al., 1985; Cordone et al., 1986). Sassaroli and Rousseau (1987) recently characterized the room temperature behavior of band III in photolyzed hemoglobin and myoglobin. Band III of photodissociated myoglobin is indistinguishable from that of deoxy-Mb within 10 ns of photolysis. However, band III of photodissociated hemoglobin is red-shifted by ~6 nm from its equilibrium deoxy position. These observations are quite consistent with results from transient optical studies (Findsen et al., 1985a,b; James et al., 1988) that have demonstrated that the heme pocket of Mb assumes its equilibrium deoxy configuration within 30 ps of ligand photolysis but the heme pocket of photodissociated hemoglobin relaxes on a much longer time scale. The relaxation kinetics of band III observed by Sassaroli and Rousseau also correlate well with heme-pocket relaxations observed in time-resolved Raman studies (Scott & Friedman, 1984). Resonance Raman studies by Scott and Friedman (1984) of the temporal evolution of ν(Fe-His) subsequent to CO photodissociation from various hemoglobins show that the relaxation of this mode to its equilibrium deoxy frequency is both species and solution dependent. Our present work demonstrates that the pH sensitivity of ligation induced changes in the protein structure are reflected in spectral changes in the 769-nm band and further suggests that these changes are related to spectral features in the time-resolved Raman spectra.

The line shape of band III also provides insight into the conformational properties of the heme pocket. Band III exhibits a Gaussian-like line shape at both low temperature (Iizuka et al., 1974; Campbell et al., 1987; Ansari et al., 1985; Fiamingo et al., 1985) and room temperature (Sassaroli, et al., 1987), suggesting that it arises from a distribution of conformations having distinct peak frequencies. Kinetic hole-burning (KHB) studies by Campbell et al. (1987) and Frauenfelder's group (Ansari, 1988) and data analysis by Agmon (1988) directly demonstrate the inhomogeneous character of band III at cryogenic temperatures. These studies suggest that the distribution of conformation-sensitive barrier heights controlling ligand binding at cryogenic temperatures is mapped onto the frequency distribution of band III. Longer wavelengths arise from the segment of the substate population

† This work supported in part by the NSF (DMB8604435) and NIH (HL13531, HLV764428 and GM33330).

* To whom correspondence should be addressed.
‡ University of New Mexico.
§ AT&T Bell Laboratories and New York University.
⊥ Present address: Department of Chemistry, Georgetown University, Washington, DC.
∥ Northwestern University.

0006-2960/90/0429-4844$02.50/0

with the lowest barriers for ligand binding. KHB studies on band III therefore allow for the probing of the functionally distinct parts of the inhomogenous population that contribute both to the band III line shape and to the distributed nature of the ligand rebinding kinetics. Furthermore, the KHB results imply that the distributed structural element(s) responsible for the inhomogenous line shape of band III is (are) intimately connected with the ligand rebinding process. Thus, the thrust of our present work is an attempt at identifying such structural elements.

The systematic and well-studied structural changes at the heme induced by tertiary and quaternary structure changes in hemoglobin provide the conformational variability necessary to examine both the general dependence of KHB on the protein structure and the possible correlations between the behavior of band III and well-characterized structure-sensitive Raman bands. We expand upon earlier cryogenic studies of band III (Campbell et al., 1987), extending them to hemoglobins and Fe–Mn hybrid hemoglobins.

Hybrid Fe–Mn hemoglobins are nearly ideal species for the study of subunit heterogeneity and protein quaternary structural influences. The Mn-containing subunits in the Mn(II) and Mn(III) valence state are structurally equivalent to the Fe subunits in the corresponding states but do not bind CO, providing a convenient avenue to study CO binding in the Fe-containing subunits. Any contributions to the absorption spectra due to the Mn-containing subunit are easily eliminated by subtraction of the unphotolyzed spectra from the photolyzed spectra, yielding exclusively band III from the five-coordinate ferrous heme. Under appropriate conditions, Fe–Mn hybrid hemoglobins can assume a T-state or an R-state configuration (Moffat et al., 1976a). This provides a means of determining the dependence of band III upon the specific tertiary structure of each subunit.

Materials and Methods

Hemoglobin was purified according to the procedure of Antonini and Brunori (1971). Deoxy samples were made by anaerobically adding a minimum amount of dithionite. Fe–Mn hemoglobin hybrids in the R state and T state were prepared according to the procedure of Blough et al. (1984). All samples were prepared with 0.1 M potassium phosphate buffer to avoid possible effects due to changes in the buffer. Samples were then brought to 75% glycerol and loaded into a 1.5-mm optical cell. Heme concentrations were typically near 1 mM. A Janis liquid helium Dewar was used to slowly freeze the sample to produce a uniform glass. Temperature control was achieved by using a Lakeshore temperature controller with a thermocouple and resistive heating. Absorption measurements were taken by using an ISA 640 single monochromator with a 600 grooves/mm grating and a Princeton Instruments OMA unintensified silicon diode array detector with data collected on an interfaced PC's Limited 286 computer. An integration time of 5 min provided a sufficient signal-to-noise ratio. The actinic light source was a regulated tungsten lamp (Newport). Photolysis was achieved by using this intense light source, and spectra were taken by using a Corning CM-52 cutoff filter and appropriate neutral density filters to minimize photolysis during data collection. Spectra of samples after partial rebinding of CO were obtained by using the procedure of Campbell et al. (1987).

To obtain the initial photoproduct, the sample was illuminated at 8 K. No detectable ligand recombination occurred at this temperature. The extent of CO recombination at elevated temperatures was calculated from the integrated area of band III. For most samples, an arbitrary temperature of 60 K was employed in order to achieve ~80% rebinding in the time span of 10 min. However, it is noteworthy that the T-state hybrids required a temperature of 140 K in order to achieve ~80% CO rebinding within 10 min. This is not surprising in view of the much lower ligand affinity of T-state hemoglobin.

Table I: Near-IR Bands of Various Hb's

species	peak (nm)	fwhm (nm)
deoxy-HbA, pH 8.0, 8 K	754.4	22.6
deoxy-HbA, pH 8.0, 160 K	755.1	22.7
deoxy-HbA, pH 6.0 + IHP, 8 K	753.8	23.3
deoxy-HbA, pH 6.0 + IHP, 180 K	754.7	22.6
deoxy-HbA, pH 7.0, 298 K	759	30.0*
HbACO, pH 8.0, 0% recombined, 8 K	763.2	20.9
HbACO, pH 8.0, 80% recombined, 8 K	763.0	20.5
HbACO, pH 6.0 + IHP, 0% recombined, 8 K	762.6	20.0
HbACO, pH 6.0 + IHP, 87% recombined, 8 K	760.4	17.1
HbACO, pH 7.0, 0% recombined, 298 K	765	30.0
$\alpha(Mn^{III})\beta(FeCO)$, pH 8.0, 0% recombined, 8 K	766.1	20.6
$\alpha(Mn^{III})\beta(FeCO)$, pH 8.0, 88% recombined, 8 K	764.4	19.2
$\alpha(Mn^{II})\beta(FeCO)$, pH 6.6 + IHP, 0% recombined, 8 K	760.8	16.0
$\alpha(Mn^{II})\beta(FeCO)$, pH 6.6 + IHP, 65% recombined, 8 K	759.2	13.2
$\alpha(FeCO)\beta(Mn^{III})$, pH 8.0, 0% recombined, 8 K	760.6	17.4
$\alpha(FeCO)\beta(Mn^{III})$, pH 8.0, 55% recombined, 8 K	760.4	17.4
$\alpha(FeCO)\beta(Mn^{II})$, pH 6.6 + IHP, 0% recombined, 8 K	758.3	18.3
deoxy-Mb, pH 7.0, 298 K	761	30.0*
MbCO, pH 7.0, 0% recombined, 8 K	764.9	16.1
MbCO, pH 7.0, 85% recombined, 8 K	760.6	15.2
MbCO, pH 7.0, 298 K	761	34.0*

Two protocols were employed to distinguish between structural relaxation and kinetic hole-burning effects on band III (Campbell et al., 1987). In protocol A, the sample was continuously illuminated during ligand rebinding at elevated temperatures (>60 K). The temperature was then lowered to 8 K and the line shape and position of band III were determined. Since rebound ligands were continuously rephotolyzed, any changes in band III could result only from structural relaxation at heme sites that have never rebound a ligand. In protocol B, ligand rebinding was allowed to proceed in the dark at elevated temperatures. Spectra of band III (at 8 K) obtained via this procedure should reveal both kinetic hole burning and relaxation (if present).

A comparison of band III spectra obtained via protocols A and B and the initial photoproduct spectrum yields the relative contributions of structural relaxation and kinetic hole burning to the position and line shape of band III. No differences were observed between protocol A and the initial photoproduct for any sample, even in the case of T-state hybrids for which the temperature was elevated to 140 K. Thus no structural relaxation was detected and changes evident on band III during protocol B are ascribed solely to kinetic hole burning.

Results

Deoxy-HbA. The characteristics of band III for deoxy-HbA were determined as a function of temperature and pH. In general, decreasing temperature produces a blue shift and an increase in the integrated intensity of band III, irrespective of sample pH. Additionally, band III for all samples at low temperatures (<180 K) displayed line shapes that were considerably narrower than those reported (Sassaroli and Rousseau, 1987) for room temperature samples (see Table I). Figure 1 demonstrates that, at 160 K, spectra of deoxy-HbA at pH 8.0 and pH 6.6 + IHP are largely equivalent (λ_{max} = 754.0 ± 0.9 nm and fwhm = 22.6 ± 0.2 nm). As the temperature is lowered to 8 K, band III of both samples shifts

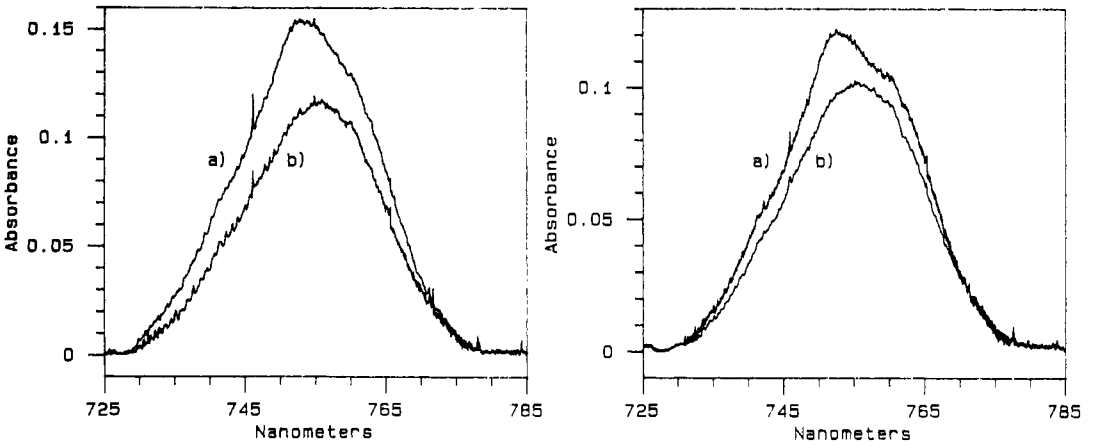

FIGURE 1: Band III of deoxy-HbA at pH 6.0 + IHP (~30 mM) and at pH 8.0 (panels on the left and right, respectively) at (a) 8 K and (b) 160 K. Hemoglobin concentration was ~5 mM (in heme). A 1.5-mm path-length cell was used and approximately 5 min of signal acquisition was required at the light levels used. The base line between 725 and 785 nm was flattened by using a quadratic fit to remove contributions for other heme transitions (most notably band IV centered at ~690 nm). See text for additional details.

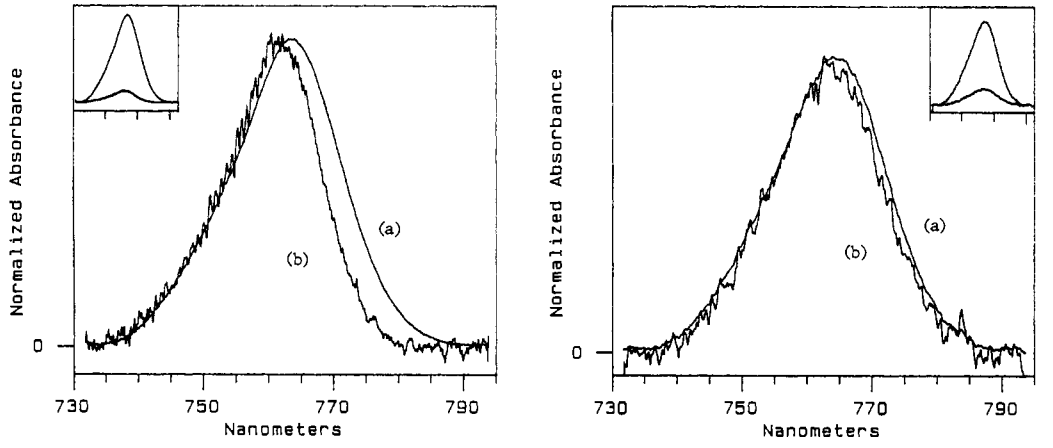

FIGURE 2: Spectra of photolyzed HbCO at pH 6.0 + IHP (left) and pH 8.0 (right). (a) Obtained from completely photolyzed samples at 8 K. (b) Results after 87% (pH 6.0) and 80% (pH 8.0) ligand recombination following protocol B (see text). Intensities of band III from rebound samples have been normalized to those of analogous completely photolyzed samples. Inserts are representative of actual absolute intensities. Other details are the same as Figure 1.

continuously to higher energy and increases in intensity. Moreover, it becomes very asymmetric, displaying two components. These effects are more pronounced for the lower pH + IHP sample.

HbACO Photoproduct and Effects of Ligand Rebinding. Peak positions of band III, for 100% photolyzed HbACO at pH 8.0 and pH 6.0 + IHP, are red-shifted relative to those of equilibrium deoxy-Hb under similar conditions. At 8 K, spectra of both photolyzed samples show a Gaussian line shape. At pH 8.0, the spectrum obtained at 8 K exhibits an absorbance maximum of 763.2 nm, whereas the sample at pH 6.0 + IHP has a maximum (762.6 nm) closer to that of equilibrium deoxy-Hb. The fwhm of band III for photolyzed HbA at pH 8.0 is 20.9 nm, 1.7 nm narrower than that of deoxy-HbA.

Spectra of HbACO (pH 8.0), obtained after partial ligand rebinding (see Figure 2), show that the effect of CO recombination on the position and line width of band III is significantly less than that exhibited by MbCO under similar conditions (Campbell et al., 1987). The change in fwhm was only 0.4 nm, and the blue spectral shift amounted to 0.2 nm when comparing 0% recombined versus 80% recombined samples. The results obtained from HbACO (pH 6.0 + IHP) are also shown in Figure 2. Under these conditions, band III exhibited substantial changes in both line shape and peak position. Decreases of 2.9 nm in fwhm and 2.2 nm in peak position were observed in the comparison of 0% recombined to 80% recombined samples. In addition, the fwhm of 80% recombined HbA at pH 6.0 + IHP was considerably narrower than that of the analogous pH 8.0 sample (see Table I).

Fe–Mn Hybrid Hb Photoproducts. Spectra of the various FeCO–MnHb hybrids, at 8 K after complete photolysis of CO, are displayed in Figure 3. The Mn(III) form of the hybrids at pH 8.0 was used to emulate the R state of HbA (see discussion below). The α- and β-Fe(II) chains within these "R-state" hybrids exhibited near-IR bands at 760.6 and 766.1 nm, respectively, suggesting a definite subunit heterogeneity in the position of the charge-transfer band. Also apparent was a difference in the fwhm. The α-Fe chain showed a fwhm of 18.5 nm, whereas the β-Fe chain showed a fwhm close to that of the photolyzed native tetramer (20.7 nm) (see Table I). Mn(II) hybrids at pH 6.6 were used in order to mimic the T-state behavior of Hb. Complete photolysis of CO from $\alpha(\mathrm{FeCO})\beta(\mathrm{Mn^{II}})$ and $\alpha(\mathrm{Mn^{II}})\beta(\mathrm{FeCO})$ yielded band III positions that were blue-shifted relative to those of the photolyzed R-state hybrids. Chain heterogeneity was also evident in these "T-state" hybrids. Under these conditions, bands III of the α-Fe chain and β-Fe chain appeared at 758.3 and 760.8 nm, respectively. The fwhm of the α chain did not change with quaternary structure, but the fwhm of the β chain narrowed from 20.7 to 16.3 nm in going from the R to T state.

The effects of CO rebinding upon band III of the photolyzed R-state hybrids $\alpha(\mathrm{Mn^{III}})\beta(\mathrm{FeCO})$ and $\alpha(\mathrm{FeCO})\beta(\mathrm{Mn^{III}})$ at pH 8.0 are shown in Figure 4. After ≈80% recombination,

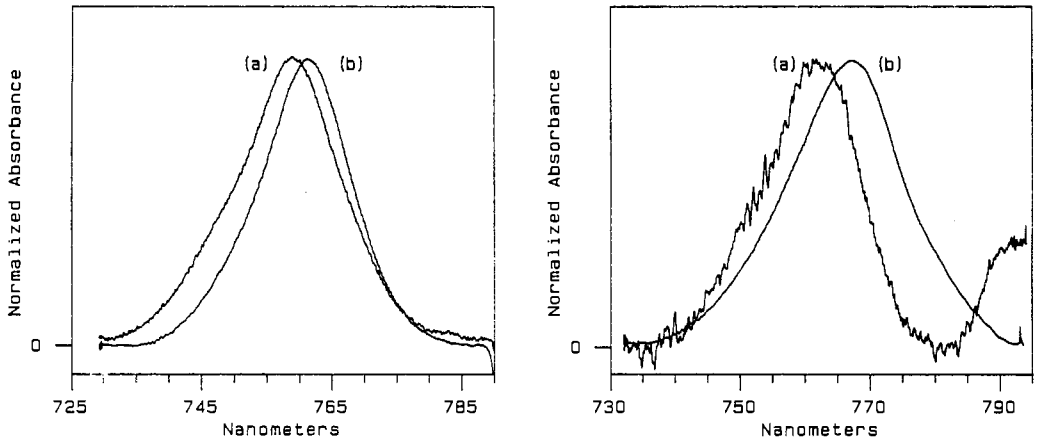

FIGURE 3: Spectra of completely photolyzed Fe/Mn hybrid hemoglobins. Left: (a) $\alpha(Fe)\beta(Mn^{II})$, (b) $\alpha(Mn^{II})\beta(Fe)$, at pH 6.6 + IHP (30 mM). Right: (a) $\alpha(Fe)\beta(Mn^{III})$, (b) $\alpha(Mn^{III})\beta(Fe)$, at pH 8.0. The feature at 780–790 nm in the right panel arises from the incomplete subtraction of a charge-transfer band from Mn^{III} subunits. Other details are the same as in Figure 1 except the concentration of the $\alpha(Fe)\beta(Mn^{III})$ sample was <1 mM in heme, while other samples were 1–2 mM.

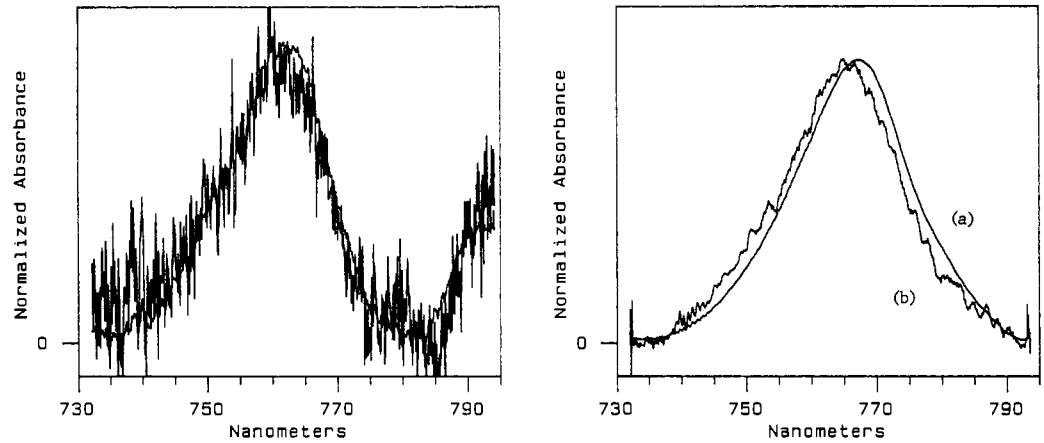

FIGURE 4: Band III of Fe/Mn hybrid hemoglobin after CO recombination at pH 8.0. Left, $\alpha(Fe)\beta(Mn^{III})$: (a) 0% recombination, (b) 80% recombination. Right, $\alpha(Mn^{III})\beta(Fe)$: (a) 0% recombination, (b) 88% recombination. Protocol B was followed. Other details are the same as in Figure 3.

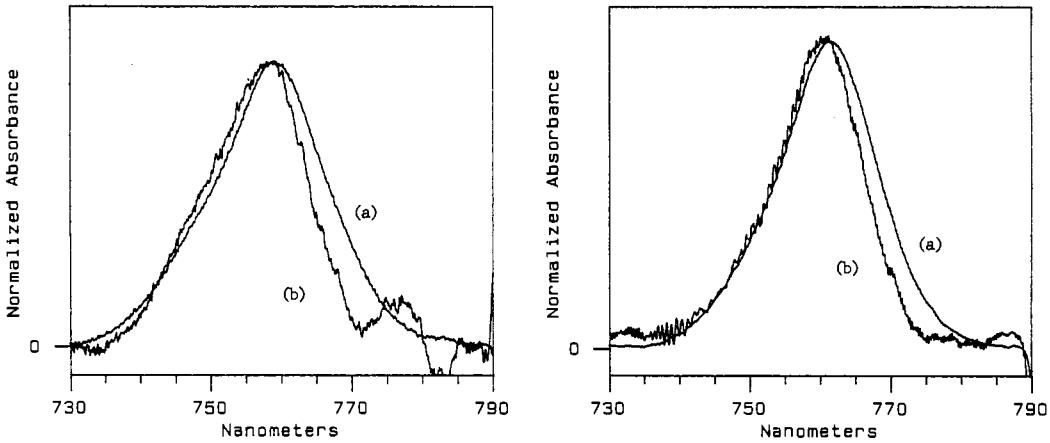

FIGURE 5: Band III of Fe–Mn hybrid hemoglobins after CO recombination at pH 6.6 + IHP (30 mM). Left, $\alpha(Fe)\beta(Mn^{II})$: (a) 0% recombination, (b) 52% recombination. Right, $\alpha(Mn^{II})\beta(Fe)$: (a) 0% recombination, (b) 55% recombination. Protocol B was followed except that the samples were raised to 140 K for 10 min to facilitate CO recombination. Other details are the same as in Figure 3.

the β(Fe) species exhibited a 1.7-nm blue shift and a 0.7-nm decrease in fwhm for band III in comparison to the initial, 0% recombined sample. On the other hand, the α(Fe) species showed much smaller differences in the position and line shape of band III after ≈80% CO recombination (see Table I).

For the T-state hybrid species, $\alpha(Mn^{II})\beta(FeCO)$ and $\alpha(FeCO)\beta(Mn^{II})$ at pH 6.6 + IHP, the rebinding of CO to the 100% photolyzed samples produced large changes in both the position and line shape of band III. These are shown in Figure 5. Under these conditions, the magnitudes of the effects on the α[Fe] and β[Fe] chains are roughly equivalent and qualitatively consistent with the increased "hole burning" exhibited by tetrameric HbA at low pH and in the presence of IHP.

Discussion

Band III arises from a porphyrin → iron charge-transfer transition; consequently, it is expected to be extremely sensitive

to the ligand field at the iron. For hemoglobins, the ligand-field parameters are directly connected to the heme-pocket structure via the Fe–proximal histidine bond. Thus, band III provides a sensitive, if indirect, indicator of alterations in the local heme-pocket geometry. Our results show that temperature, protein tertiary and quaternary structure, chain type, and ligand rebinding subsequent to photolysis all affect the position and line width of band III.

Temperature Dependence of Band III in Deoxy-Hb. The 760-nm transition for deoxy-HbA shows a dramatic dependence upon temperature for samples at both pH 8.0 and pH 6.0 + IHP. Two effects are apparent as the temperature is lowered to 8 K: an overall increase in the oscillator strength of band III and the separation of the overall line shape into two discernible bands. These can be attributed to both general and chain-specific alterations in the heme pocket as a function of temperature.

The overall increase in the extinction coefficient of band III as a function of temperature has been reported by Cordone et al. (1986). The increase in the oscillator strength of band III exceeds 15% for all samples examined. This strongly suggests that specific alterations of the heme-pocket geometry occur in deoxy-Hb as the temperature is lowered. The general origin of these structural changes most likely involves the contraction of the heme pocket at cryogenic temperatures. Nonuniform internal protein contractions of ~3% were seen by Frauenfelder et al. (1987) in analyzing the refined X-ray crystal structures of myoglobin at 80 and 255–300 K. These contractions could modulate the energy of the charge-transfer band by influencing the electronic overlap of the relevant molecular species.

Cordone et al. (1986) proposed that a decrease in the iron displacement from the heme plane, resulting from a decrease in temperature, could lead to a more enhanced π overlap and, thus, a higher extinction coefficient. Recent cryogenic Raman studies of hemoglobins and myoglobins (Bangcharoenpaurpong et al., 1984; Ondrias et al., 1983a) offer some insight into the specific effects of low temperature upon the heme–histidine geometry. For hemoglobins, the Fe–His stretching mode increased in frequency as the temperature was lowered. However, variations in the intensity of ν(Fe–His) with temperature and excitation frequency could not be modeled solely on the basis of Fe–His bond strength. Bangcharoenpaurpong et al. (1984) theorized that changes in the azimuthal rotation of the proximal histidine can lead to changes in both frequency and intensity in ν(Fe–His). More recently, a model has been proposed (Friedman et al., 1990) that links the resonance enhancement of ν(Fe–His) with heme–histidine π overlap (modulated by the protein controlled histidine azimuthal angle) and the frequency of ν(Fe–His) to the σ bonding between the Fe and histidine (affected primarily by the histidine tilt angle). In this scenario, it is possible for a given intrinsic Fe–His bond strength (i.e., frequency of ν(Fe–His)) to be associated with varying degrees of heme–histidine π overlap by varying the azimuthal angle. The frequency of ν(Fe–His) is correlated with the determinants of quaternary structure [see Rousseau and Friedman (1988)]. This correlation leads to a model in which the $\alpha_1\beta_2$ interface controls the histidine tilt through the F helix [see Rousseau and Friedman (1988) for a discussion]. For a given $\alpha_1\beta_2$-determined histidine tilt, there can then exist a distribution of azimuthal angles for the histidine that is modulated both by the degree of tilting and by the architecture of the proximal heme pocket. Due to enhanced repulsive interactions a more tilted configuration would bias the rotational distribution away from rotational conformations that have the F8 imidazole eclipsing the iron–pyrrole nitrogen axis.

Band III is likely to be sensitive to both forms of modulation of heme–histidine interactions. Tilting of the Fe–His bond would destabilize the Fe d_π orbital relative to the porphyrin a_{1u} and a_{2u} orbitals, producing a blue shift in band III. Changes in the spatial overlap of these orbitals, and hence the band III oscillator strength, are undoubtedly strongly coupled to Fe–histidine geometry. The general contraction of the heme pocket at cryogenic temperatures may generate the observed temperature-dependent behavior of band III.

It is anticipated that more specific variations in local heme-pocket structure will further modulate the spectroscopic effects of heme-pocket contraction. Our data show that changes in pH, binding of allosteric effectors, and differences between α and β chain all affect band III. Band III of deoxy-Hb clearly separates into two components (see Figures 1 and 2) as the temperature is lowered to 8 K, irrespective of the initial solution conditions (pH and the presence of IHP). In all instances, the higher energy band exhibits a pronounced increase in relative intensity as the temperature is lowered, causing a net blue shift of the overall composite band. On the basis of the spectra of the photolyzed Fe–Mn hybrid hemoglobin (see below), we attribute the origin of the high-energy band to the α-Fe chains and the lower energy band to the β-Fe chains.

Subunit Heterogeneity in Deoxy-HbA. Ample precedent exists for spectroscopic differences between the α chain and β chain. Various Raman studies [see Rousseau and Friedman (1988) for a review] have demonstrated that α,β-chain heterogeneity is evident in the heme pockets of hemoglobins and hybrid hemoglobins (Ondrias et al., 1982) at equilibrium. For instance, the α-Fe chain of T-state Fe/Co hybrids exhibits a ν(Fe–His) at 201 cm^{-1} with a shoulder at 212 cm^{-1}, whereas, in the corresponding β-Fe chain, ν(Fe–His) is more intense and higher in energy (218 cm^{-1}). Thus, the putative heme-pocket contraction at low temperatures might well produce differential effects in the spectra of band III from α and β chains. Our data analysis is consistent with larger temperature effects in the α heme pocket than the β heme pocket. It is also noteworthy that the pH 6.0 + IHP samples exhibited greater temperature variations in both components of band III than the pH 8.0 samples. Protein tertiary structure is seemingly a major factor in determining band III characteristics.

Cryogenically Trapped Photoproducts. Observation of a significant (~10 nm) shift to lower energy for band III of the cryogenically trapped HbA photoproduct species, relative to their deoxy-HbA counterparts, is qualitatively consistent with other spectroscopic data. In particular, shifts of this magnitude have been observed in band III of HbCO photolytic transients at room temperature (Sassaroli and Rousseau, 1987). The subsequent evolution of band III to its equilibrium position was correlated with the previously observed time-dependent behavior of ν(Fe–His) of the phototransient species (Scott & Friedman, 1984).

Photolysis of CO from HbCO instantaneously ($\ll$30 ps) produces a nonequilibrium active site. The heme itself relaxes to an equilibrium deoxy state on a 30-ps time scale or faster (Findsen et al., 1985), while the surrounding heme pocket exhibits a much slower nanosecond and longer evolution to its equilibrium deoxy configuration (Scott and Friedman, 1984). At cryogenic temperatures, it is possible to completely suppress heme-pocket structural relaxation. Thus, our spectra are reflective of the high-spin, five-coordinate heme within a "ligated" protein configuration and those heme-pocket dy-

namics that do not require large-scale protein structural relaxation. The characteristics of band III under these conditions provide insight into the initial heme-pocket dynamics that precede the nanosecond and longer protein structural relaxations.

The shifts in band III of the photoproduct species are consistent with changes in the Fe–proximal histidine geometry (see above). Previous resonance Raman studies of Hb phototransient species have shown that the "unrelaxed" ligated heme pocket invariably results in a higher frequency for ν(Fe–His) than that seen in the "relaxed" deoxy species (Rousseau and Friedman, 1988). This behavior has been interpreted to result largely from a more perpendicular orientation of the proximal histidine with respect to the heme plane. This orientation would also be expected to minimize repulsive interactions between Fe d_π and ligand orbitals, lowering the energy of the CT band (see above).

Ligand photolysis results in transient species exhibiting band III line widths that are narrower than those of the equilibrium deoxy species. Further narrowing is observed for the photoproduct in going from pH 8 to pH 6 + IHP. It is possible that this narrowing of band III reflects a more restricted distribution of conformational substates induced by ligand binding and pH changes. This possible interpretation is predicated on the premises that the spectrum of the frozen photoproduct reflects the structure of the initial liganded species and the interconversion or relaxation of conformational substates is expected to be essentially zero at 8 K. A narrower distribution of substates for the liganded structure is consistent with an earlier analysis of heme $\pi\pi^*$ transitions (Srajer et al., 1986). An obvious complication in the analysis of the line narrowing in hemoglobin is the possibility of subunit heterogeneity obscuring other sources of line-shape changes. To complete any such analysis of hemoglobin it is, of course, necessary to assign the peak wavelength positions and line-shape contributions to the specific subunits as a function of tertiary structure. The mixed-metal hybrids provide the means to this end.

1. Subunit Heterogeneity in Fe–Mn Hybrids. Subunit heterogeneity can be seen directly in properties of band III for the photolyzed Fe–Mn(III) hybrids. Various studies (Moffat et al., 1976a; Hoffman et al., 1975) have revealed that the Fe–Mn(III) hybrids mimic R-state HbA intermediates. The behavior of band III of the photolyzed α and β ferrous subunits corroborates these findings. The position and line width of band III of photolyzed tetrameric HbA are closely approximated by summing spectra of the individual α and β chains of the photolyzed R-state hybrids. The characteristics of band III in these species do, however, reveal significant subunit heterogeneity. Our data show that the peak position of band III for the five-coordinate ferrous α-chain photoproduct is substantially blue-shifted relative to the β-chain peak (see Figure 4). It is also apparent that band III of the photolyzed ferrous α chains is narrower than those of either photolyzed tetrameric HbA or the photolyzed β chains (see Table I). Nonetheless, both chains display considerable inhomogeneity in band III and, by inference, their proximal heme pockets.

Data obtained from Fe–Mn hybrid hemoglobins indicate that band III is also sensitive to the quaternary structure of the tetramer. Analysis of the liganded T-state structure is not possible with HbA under any known solution conditions. However, structural studies (Gonzales, et al., 1975) of the tetrameric MnHb revealed that the Mn(II)-containing subunits displayed properties identical with those of unliganded Fe(II) subunits. Therefore, Fe–Mn(II) hybrid hemoglobins provide an analogue to T-state hemoglobins that have only two bound CO molecules. Moreover, Blough et al. (1980) showed that the ligand binding kinetics of Fe–Mn(II) hybrids at pH 6.6 + IHP are very similar to those of native T-state tetramers. The present results indicate that the R/T quaternary transition has a much larger effect upon the proximal pocket of the photoproduct β chains than on the photoproduct α chains. Band III of photolyzed T state from $\alpha(Mn^{II})\beta(FeCO)$ (pH 6.6 + IHP) is significantly narrower and blue-shifted relative to that of photolyzed R state from $\alpha(Mn^{III})\beta(FeCO)$ (pH 8.0). On the other hand, CO photolysis from analogous T- and R-state α(Fe) hybrids yields nearly equivalent widths and only slightly shifted peak positions for band III. Since it is not likely that the variability in the line width of band III is due to changes in excited-state lifetime or dephasing time of the transition, it is probable that it results from an R/T-sensitive change in the conformational disorder of the proximal heme pocket within the β-subunit photoproduct.

The changes in band III between the deoxy T state and the half-liganded T state parallel structural differences observed by X-ray crystallography. X-ray diffraction studies by Arnone et al. (1986) on $[\alpha(FeCO)\beta(Mn^{II})]_2$ have revealed that this tetramer has a T-state structure even though it is half-liganded. Subtle differences were observed when comparing this hybrid to the deoxyhemoglobin. In particular, the iron atom is drawn into the heme plane and consequently the last turn of the F helix moves closer to the heme group upon CO binding to the α subunit of the hybrid. Since the protein tertiary structure is frozen in at 10 K, the differences in the peak position of band III for the deoxy and T-state photoproduct species should reflect those changes observed in the above crystallographic studies.

The subunit-specific behavior of band III in deoxy, liganded, and partially liganded structures reveals fundamental differences in the heme-pocket dynamics of α and β subunits. Band III for deoxy-HbA at 8 K shows two peaks that can be attributed to the α and β subunits. The α component is at ~753 nm, whereas the β component is at ~760 nm. Thus, in going from deoxy-T to liganded-T photoproduct to liganded-R photoproduct band III for the α subunit goes from 753 to 758.3 to 760.6 nm, respectively, and for the β subunit it goes from 760 to 760.8 to 766.1 nm, respectively. It is interesting that major tertiary structural changes in the α subunits apparently occur both upon ligand binding within the T quaternary state and upon the subsequent change in quaternary state. In contrast major changes occur in the β subunits only upon going from liganded-T to liganded-R configurations.

In this respect, the behavior of band III is very similar to the behavior observed for ν(Fe–His) in the transient Raman spectra of photolyzed HbCO at ambient temperatures [see Rousseau and Friedman (1988) for a review]. As the heme pocket evolves from liganded-R photoproduct to liganded-T photoproduct to deoxy T, the frequency of the composite ν(Fe–His) band shifts from 230 to ~220 to 215 cm^{-1}. The resonance Raman studies of hybrid hemoglobins (Rousseau & Friedman, 1988; Kaminka et al., 1989; Scott et al., 1983) have shown that ν(Fe–His) of the α subunit goes from 230 to ~220 to ~205 cm^{-1}. The β subunit shifts from 230 to ~220 to 218 cm^{-1}, respectively, with the middle value being inferred. These patterns of change are very similar to the chain-specific behavior observed for band III.

In spite of the similarities in the subunit specific responses of band III and ν(Fe–His) to protein tertiary structure, there is a potentially important difference. For band III the α and β subunits never occur at the same position for a given ter-

tiary–quaternary state of the protein. The frequency of ν(Fe–His) in photoproduct transient species is, however, the same for α and β subunits for the pH 8 R-state structure (Scott et al., 1983). This difference strongly suggests that the position of band III is sensitive to structural parameters that are not reflected in the frequency of ν(Fe–His) (see below).

2. Influence of Ligand Rebinding. A distribution of barrier heights controlling ligand binding has been postulated in order to account for the power law kinetics observed for heme proteins at cryogenic temperatures (Austin et al., 1975). In this model, different conformational substates of the protein can have different functional properties. At higher temperatures, rapid interconversion among substates leads to a time-averaged structure with simple, first-order kinetics; however, at sufficiently low temperatures, each molecule is trapped within a specific substate and therefore has a distinct kinetic rate constant.

If there is a simple relationship between heme-pocket structure within protein conformations and band III, with some conformations rebinding faster than others, the line shape could be time dependent, reflecting the changing distribution of conformations as rebinding proceeds. Campbell et al. (1987), Agmon (1988), and Ansari (1988) have shown that band III of photolyzed myoglobin exhibits precisely this type of inhomogeneous behavior during CO rebinding at cryogenic temperatures. Our data demonstrate that hemoglobin also exhibits kinetic hole-burning behavior. The similarity between Hb and Mb with respect to the general magnitude of the KHB effect indicates that as for Mb the line shape of band III for Hb is dominated by a large homogeneous contribution that limits the extent of hole burning (Agmon, 1988; Ansari, 1988). The magnitude of this effect in Hb is, however, dependent upon many factors that modulate the heme-pocket tertiary structure.

Figure 2 clearly shows that, under pH 6.0 + IHP conditions, ligand rebinding to photolyzed HbA proceeds faster at those heme sites that have lower energy positions for band III. This behavior is similar to that of photolyzed Mb and indicates that a distribution of barriers to ligand rebinding maps onto the line shape of band III. Within the context of our rebinding analysis, this mapping links the distributed rebinding kinetics to conformational heterogeneity within the proximal heme pocket. Thus, we conclude that, under low-pH conditions, the lower energy components in the band III profile correspond to heme sites in proximal heme-pocket conformations having lower barriers to recombination.

Photolyzed carbonmonoxy-HbA at pH 8.0 exhibits little or no kinetic hole burning upon ligand rebinding. This finding is somewhat surprising in light of the results from the comparable sample at pH 6.0 + IHP. At elevated pH it appears that there is less of a mapping of rebinding rates onto line shape than at lower pH values. Analogous behavior is seen in the Fe/Mn hybrids (Figures 4 and 5) and in tuna HbCO under high-pH (R-state) and low-pH (T-state) conditions (Campbell and Friedman, unpublished results). In these cases, kinetic hole burning is much more evident in the T-state species. These results all suggest a trend in which the more T-like structures exhibit a greater extent of kinetic hole burning.

Three possible explanations for this pH-dependent trend in the extent of hole burning include (1) a substantial pH dependence of the homogeneous width of band III such that at high pH the homogeneous contribution to the line shape dominates; (2) a distribution of sufficiently low rebinding barriers at high pH, which results in a loss in substate selectivity at the temperatures used to initiate rebinding; and (3) a pH-dependent change in the sensitivity of the recombination process to the structural parameter responsible for the inhomogeneous broadening of band III.

Although there is some precedent for a dependence of heme excited-state lifetimes on protein structure (Friedman et al., 1977), possibility 1 seems unlikely on the basis of the absence of line narrowing for the α subunits in going from the R to T structures. A study on carp hemoglobin (Coban et al., 1985) shows that at cryogenic temperatures the R structure has a distribution of recombination barriers that is lower than those within the T-state distribution; none the less, explanation 2 is still unlikely given the temperatures required to produce partially recombined samples having R, T, and strained-R structures. Although it is not possible to categorically dismiss the first two explanations for the pH dependence, the structural model discussed in the next section provides support for the third explanation (vide infra).

Spectra, Structure, and Function

The results of this study are consistent with the earlier claims that band III is inhomogeneously broadened by a distributed degree of freedom that is either the cause of the distributed kinetics or is intimately coupled to whatever is the causal degree of freedom.

Clearly many factors can influence the electronic transitions giving rise to band III. Of these, several including the electrostatic and dielectric influences of the protein can no doubt be linked to reactivity. However, the direct involvement of the iron in this transition, the proposed key role of the iron in modulating ligand-binding reactivity, and the earlier interpretation of inhomogeneous line broadening in terms of the distribution of iron displacements (Srajer, et al 1988) make the iron and the determinants of the iron displacement from the heme plane the obvious first focus of any study explaining the structural basis of the KHB band in III. Proximal strain is usually invoked as the link between the protein tertiary and quaternary structure and the displacement of the heme iron. Extensive resonance Raman studies indicate that the frequency of ν(Fe–His) in stable and transient (photoproduct) forms of deoxy-Hb and deoxy-Mb reflects this proximal strain (Friedman, 1985; Roussean & Friedman, 1988). Consequently, the observed similarities in the behavior of band III and ν(Fe–His) are certainly a basis for exploring a possible structural explanation for the behavior of band III. The obvious questions are what is the identity of this structural degree of freedom, how does it modulate ligand binding, and by what mechanism does it influence band III? The similarity in the behaviors of ν(Fe–His) and band III in response to structural changes associated with ligand binding suggests that the iron and its immediate environs play critical roles in the energetics of ligand binding.

The frequency response of ν(Fe–His) to protein structure and the correlation of this frequency with ligand-binding properties have led to the proposal that the protein-controlled tilt of the proximal histidine (in its own plane) with respect to the heme plane is the parameter that modulates both Raman frequency and ligand-binding barrier height. The more T-like the protein structure, the greater is the tilt of the histidine. The increase in tilt weakens or strains the Fe–His bond and favors a more out-of-plane iron. These protein-induced changes result from an increase in the nonbonded repulsive interaction between the pyrrole nitrogens and the imidazole carbons, which also makes it energetically more costly to move the iron into the heme plane upon ligand binding. The tilt of the histidine is also a strong candidate for the structural parameter modulating the position of band III. Changing the

tilt would affect the displacement of the iron and thereby alter the π coupling between the iron and the porphyrin. Such a change would alter the energy of the change-transfer transition that gives rise to band III. Thus, the inhomogeneous distribution of wavelength for band III could arise from a distribution of iron displacements.

Insofar as the tilt of the histidine has a direct correspondence with the frequency of ν(Fe–His), there must be additional factors influencing band III. The frequency of ν(Fe–His) is the same for α and β subunits in the pH 8 photoproduct (Scott et al., 1983) whereas the corresponding peak positions of band III are different. It is possible that the comparison between a liquid solution (for the Raman) and a cryogenic glass is not meaningful in this instance. Alternatively, the azimuthal angle of the histidine is not expected to have a strong influence on the σ character of the Fe–His bond but is capable of influencing π interactions between the metal and the macrocycle (Scheidt and Chapman, 1986). The frequency of ν(Fe–His) is most directly a measure of the σ character of the bond. Thus, the azimuthal angle of the histidine should have little effect on the ν(Fe–His) frequency but can still exert influence on the peak positions of band III.

The azimuthal angle of histidine F8 can also contribute to the height of the recombination barrier under the following conditions: (1) Tilting the histidine favors the noneclipsed conformations of the imidazole ring (with respect to the iron–pyrrole nitrogen axis). Conversely, for an untilted geometry there is less of an energy difference among rotational conformations of the imidazole. (2) For a given tilt angle of the histidine, the more eclipsed imidazole–heme conformation (closer to a 0° azimuthal angle) produces a greater barrier for ligand binding.

Thus if the architecture of the proximal heme pocket allows for a distribution of azimuthal angles, then the T-like tertiary structures (increase in the tilt of the histidine) should produce a narrower rotational distribution but with greater functional distinction among the rotational conformations.

We attribute the pH-induced shifts in the peak position of band III to changes in the histidine tilt and the bulk of the inhomogeneous broadening to a distribution of rotational conformations of the His (F8) imidazole. This provides a consistent picture that accounts for the pH dependence of both the line width and the kinetic behavior of band III. At high pH, band III for the HbA photoproduct is maximally shifted to the red and displays the maximum inhomogeneous width because an untilted histidine–heme geometry minimizes the energy differences among the different accessible rotational substates of the histidine. The reduction in kinetic hole burning at high pH results from the absence of substantial functional differences among the members of the distribution of rotational substates when the proximal histidine is upright. The properties of the low-pH (+IHP) band III (vis-à-vis pH 8) are attributable to a skewing of the distribution of rotational substates away from the more eclipsed conformations due to the increased tilting of the heme–histidine configuration. The variation in rebinding kinetics for the distribution of azimuthal angles is increased and kinetic hole burning is now observed at low temperatures.

Conclusion

Several key conclusions can be derived from the present study. The wavelength of band III is structure sensitive. The position of band III changes in response to those tertiary and quaternary changes that are also known to change the frequency of ν(Fe–His) in the Raman spectrum. The overall line shape of band III is derived both from subunit heterogeneity and from conformational disorder within each subunit. As observed earlier with myoglobin, those conformations having the redder wavelengths for band III tend to have the lowest barrier for recombination. A model is suggested that relates ligand binding kinetics to specific structural aspects of the proximal heme pocket. In this model, conformational degrees of freedom of the heme–histidine (F8) unit are directly connected with both the peak position and line shape of band III. Protein-induced changes in the peak positions of band III are attributed primarily to a change in the tilt of proximal histidine with respect to the heme plane, whereas changes in line shape originate largely from a "tilt"-sensitive distribution of rotational conformers of the His (F8) imidazole. The extent to which this conformational heterogeneity has functional manifestations varies with the pH- and quaternary-structure-dependent geometry of the proximal heme pocket.

References

Agmon, N. (1988) *Biochemistry 27*, 3507–3511.

Ansari, A. (1988) Thesis, Department of Physics, University of Illinois, Urbana, IL.

Ansari, A., Berendzen, J., Bowne, S. F., Frauenfelder, H., Iben, I. E. T., Sauke, T. B., Shyamsunder, E., & Young, R. D. (1985) *Proc. Natl. Acad. Sci. U.S.A. 82*, 5000–5004.

Antonini, E., & Brunori, M. (1971) *Hemoglobin and Myoglobin and Their Reaction with Ligands*, pp 2–4, Elsevier, New York.

Arnone, A., Rogers, P., Blough, N. V., McGourty, J. L., & Hoffman, B. M. (1986) *J. Mol. Biol. 188*, 693–706.

Austin, R. H., et al. (1975) *Biochemistry 14*, 5355–5375.

Bangcharoenpaurpong, O., Schomacker, K. T., & Champion, P. M. (1984) *J. Am. Chem. Soc. 106*, 5688–5698.

Blough, N. V., & Hoffman, B. M. (1984) *Biochemistry 23*, 2875–2882.

Blough, N. V., Zemel, H., Hoffman, B. M., Lee, T. C. K., & Gibson, Q. H. (1980) *J. Am. Chem. Soc. 102*, 5683–5685.

Campbell, B. F., Chance, M. R., & Friedman, J. M. (1987) *Science (Washington, D.C.) 238*, 373.

Coban, W. G., LeGrange, J. D., & Austin, R. H. (1985) *Biophys. J. 47*, 781.

Cordone, L., Cupane, A., Leone, M., & Vitrano, E. (1986) *Biophys. Chem. 24*, 259–275.

Eaton, W. A., & Hofrichter, J. (1981) *Methods Enzymol. 76*, 175–261.

Eaton, W. A., Hanson, L. K., Stephens, P. J., Sutherland, J. C., & Dunn, J. B. R. (1978) *J. Am. Chem. Soc. 100*, 4991–5003.

Fiamingo, F. G., & Alben, J. O. (1985) *Biochemistry 24*, 7964–7970.

Findsen, E. W., Scott, T. W., Chance, M. R., Friedman, J. M., & Ondrias, M. R. (1985a) *J. Am. Chem. Soc. 107*, 3355–3357.

Findsen, E. W., Friedman, J. M., Ondrias, M. R., & Simon, S. R. (1985b) *Science (Washington, D.C.) 229*, 661–665.

Frauenfelder, H., Hartmann, H., Karplus, M., Kuntz, I. D., Jr., Kuriyan, J., Parak, F., Petsko, G. A., Ringe, D., Tilton, R. F., Jr., Connolly, M. L., & Max, N. (1987) *Biochemistry 26*, 254–261.

Friedman, J. M. (1985) *Science (Washington, D.C.) 228*, 1273–1280.

Friedman, J. M., Rousseau, D. L., & Adar, F. (1977) *Proc. Natl. Acad. Sci. U.S.A. 74*, 2607–2611.

Friedman, J. M., Campbell, B. F., & Noble, R. (1990) *Biophys. Chem.* (in press).

Gingrich, D. J., Nocek, J. M., Martin, G. S., & Hoffman, B. M. (unpublished results).

Gonzales, B., Loula, J., Lee, S., Reed, J. F., Kirner, J. F., & Scheidt, W. R. J. (1975) *J. Am. Chem. Soc. 97*, 3247-3249.
Hoffman, B. M., Gibson, O. H., Bull, C., Crepeau, R. H., Edelstein, S. J., Fisher, R. G., & McDonald, M. J. (1975) *Ann. N.Y. Acad. Sci.*, 174-186.
Iizuka, T., Yamamoto, H., Kotani, M., & Yonetani, T. (1974) *Biochim. Biophys. Acta 371*, 126-139.
James, S. M., Dalickas, G. A., Eaton, W. A., & Hochstrasser, R. M. (1988a) *Biophys. J. 54*, 545-550.
James, S. M., Dalickas, G. A., Eaton, W. A., & Hochstrasser, R. M. (1988b) *Biophys. J. 54*, 545-550.
Kaminaka, S., Ogura, T., Kitagishi, K., Yonetani, T., & Kitagawa, T. (1989) *J. Am. Chem. Soc. 111*, 3787-3794.
Moffat, K., Loe, R. S., & Hoffman, B. M. (1976) *J. Mol. Biol. 104*, 669-685.
Morris, R. J., & Gibson, Q. H. (1982) *J. Biol. Chem. 257*, 4869-4874.
Ondrias, M. R., Rousseau, D. L., Kitagawa, T., Ikeda-Saito, M., Inubishi, T., & Yonetani, T. (1982) *J. Biol. Chem. 257*, 8766-8700.
Ondrias, M. R., Rousseau, D. L., & Simon, S. R. (1983) *J. Biol. Chem. 258*, 5638.
Rousseau, D. L., & Friedman, J. M. (1988) *Biological Applications of Raman Spectroscopy*, pp 135-215, John Wiley & Sons, New York.
Sassaroli, M., & Roussean, D. L. (1987) *Biochemistry 26*, 3092.
Scheidt, W. R., & Chapman, D. M. (1986) *J. Am. Chem. Soc. 108*, 1163-1167.
Scott, T. W., Friedman, J. M., Ikeda-Saito, M., & Yonetani, T. (1983) *FEBS Lett. 158*, 68-72.
Scott, T. W., & Friedman, J. M. (1984) *J. Am. Chem. Soc. 106*, 5677-5687.
Srajer, V., Schomaker, K. T., & Champion, P. M. (1986) *Phys. Rev. Lett. 57*, 1276-1270.
Srajer, V., Reinisch, L., & Champion, P. M. (1988) *J. Am. Chem. Soc. 110*, 6656-6666.

Purification and Characterization of Annexin Proteins from Bovine Lung†

Navin C. Khanna, Earl D. Helwig, N. Wayne Ikebuchi, Sandra Fitzpatrick, Ravinder Bajwa, and David M. Waisman*

Cell Regulation Group, Department of Medical Biochemistry, University of Calgary, Calgary, Alberta, Canada T2N 4N1

Received September 14, 1989; Revised Manuscript Received January 17, 1990

ABSTRACT: Calcium-dependent association with a detergent-extracted particulate fraction was used as the first step in the purification of a group of phospholipid binding proteins. Elution of the detergent-insoluble fraction with excess ethylene glycol bis(β-aminoethyl ether)-*N*,*N*,*N*′,*N*′-tetraacetic acid (EGTA) resulted in the release of several soluble proteins, termed calcium-activated proteins or CAPs. In the present paper, we describe the simultaneous purification of these CAPs and characterize their interaction with phospholipid, actin, and calmodulin. Partial sequence analysis has identified the majority of the CAPs as members of the annexin family of calcium and phospholipid binding proteins. Two additional CAPs may be novel proteins, one of which appears to be an annexin protein. All CAPs demonstrated Ca^{2+}-dependent binding to phosphatidylserine vesicles but did not bind to phosphatidylcholine vesicles. The majority of CAPs exhibited Ca^{2+}-dependent binding to F-actin; however, only CAP-III affected the rate of conversion of G-actin to F-actin. The interaction of CAP-III and lipocortin-85 with F-actin resulted in a Ca^{2+}-dependent increase in both light scattering and sedimentation of F-actin under comparatively low centrifugal force. In contrast, only lipocortin-85 caused the formation of F-actin bundles. Although all of the CAPs bound to a calmodulin affinity column in a Ca^{2+}-dependent manner, attempts to demonstrate binding of CAPs to native calmodulin were unsuccessful. These studies therefore document the similar behavior of the CAPs toward phospholipid and calmodulin but clearly show that F-actin binding or bundling is not a general property of these proteins. The reported purification procedure should allow further comparative studies of these proteins.

Over the last few years, several laboratories interested in the role of calcium in the regulation of secretion and cell motility have identified a family of Ca^{2+} binding proteins distinct from the "EF domain" group of proteins [for reviews, see Klee (1988), Khanna et al. (1988), Crompton et al. (1988a), Dedman (1986), Geisow et al. (1988), and Glenney (1988)]. These proteins have been identified on the basis of their Ca^{2+}-dependent binding to membrane fractions and elution in the absence of Ca^{2+}. The membrane fractions used for isolation of these proteins have included chromaffin granule membranes [the ethylene glycol bis(β-aminoethyl ether)-*N*,*N*,*N*′,*N*′-tetraacetic acid (EGTA)[1]-eluted proteins were called chromobindins; Creutz, 1981; Geisow & Burgoyne, 1982], the intestinal epithelial cell (the EGTA-eluted proteins were called proteins I-III; Gerke & Weber, 1985), smooth muscle membranes (Raeymaekers et al., 1985), liver (one of the mem-

† Supported by a grant from the Medical Research Council of Canada and the Alberta Heritage Foundation for Medical Research.
* Address correspondence to this author.

[1] Abbreviations: EGTA, ethylene glycol bis(β-aminoethyl ether)-*N*,*N*,*N*′,*N*′-tetraacetic acid; PI, phosphatidylinositol; PS, phosphatidylserine; PE, phosphatidylethanolamine; PC, phosphatidylcholine; PA, phosphatidic acid; CAP, calcium-activated protein; DTT, dithiothreitol; SDS, sodium dodecyl sulfate; PAGE, polyacrylamide gel electrophoresis; TFA, trifluoroacetic acid; HPLC, high-pressure liquid chromatography; MOPS, 3-(*N*-morpholino)propanesulfonic acid.

0006-2960/90/0429-4852$02.50/0